

Should we pre-train a decoder in contrastive learning for dense prediction tasks?

Sébastien Quetin^{*1}, Tapotosh Ghosh^{*2}, Farhad Maleki²
¹ McGill University ² University of Calgary

Abstract

*Contrastive learning in self-supervised settings primarily focuses on pre-training encoders, while decoders are typically introduced and trained separately for downstream dense prediction tasks. This conventional approach, however, overlooks the potential benefits of jointly pre-training both the encoder and decoder. In this paper, we propose **DeCon**: a framework-agnostic adaptation to convert an encoder-only self-supervised learning (SSL) contrastive approach to an efficient encoder-decoder framework that can be pre-trained in a contrastive manner. We first update the existing architecture to accommodate a decoder and its respective contrastive loss. We then introduce a weighted encoder-decoder contrastive loss with non-competing objectives that facilitates the joint encoder-decoder architecture pre-training. We adapt two established contrastive SSL frameworks tailored for dense prediction tasks, achieve new state-of-the-art results in COCO object detection and instance segmentation, and match state-of-the-art performance on Pascal VOC semantic segmentation. We show that our approach allows for pre-training a decoder and enhances the representation power of the encoder and its performance in dense prediction tasks. This benefit holds across heterogeneous decoder architectures between pre-training and fine-tuning and persists in out-of-domain, limited-data scenarios.*

1. Introduction

The increasing demand for efficient Deep Learning (DL) methods arises from their ability to address complex tasks. While traditional approaches like supervised learning can yield powerful, high-performing models, they depend heavily on large volumes of high-quality labeled data. However, obtaining such annotations is often tedious, expensive, and sometimes impractical, even when abundant data is available. To overcome this bottleneck, one can benefit from a pre-trained model. Pre-trained models are usually models trained from scratch on a large scale dataset

^{*}Equal contributions for this work. Co-first authors are ordered in alphabetical order.

and allow for better performance on downstream tasks with smaller datasets. Typically, an encoder is pre-trained to capture a representation of the input data, which can then be fine-tuned for downstream tasks such as classification or segmentation. During the downstream fine-tuning phase, randomly initialized layers are typically added on top of the encoder, and the complete architecture is retrained using a supervised learning approach on part of or on a full annotated dataset. ImageNet [15] is a large and widely utilized dataset with annotated classes. However, models pre-trained on ImageNet classification are not the best fit for every downstream tasks, especially when the downstream objective is not classification. Since creating large-scale annotated dataset for every tasks presents numerous challenges, Self-Supervised Learning (SSL) has emerged as a promising alternative, enabling models to learn from the vast amount of unlabeled data and perform effectively on various downstream tasks. These pre-trained models can reach downstream performance close to a fully supervised approach using much smaller to no labeled datasets. Notable approaches such as SimCLR [7], VicReg [2], and MoCo [22] showed promising results by leveraging contrastive learning for downstream classification. However, most SSL frameworks primarily target classification downstream tasks. Some efforts such as PixCon [37] or DenseCL [45], focus on dense prediction tasks like segmentation or object detection. In all of these efforts, authors only train the encoders of the DL architectures and focus on incorporating a local loss with existing classification-targeted SSL approaches to adapt with dense tasks.

In this work, we propose a **Decoder-aware contrastive learning (DeCon)** approach, a framework agnostic encoder-decoder adaptation to pre-train an encoder jointly with a decoder, improving its representation power and efficiently preparing it to be combined with a decoder in downstream tasks. Our contributions are as follows.

- We propose **DeCon-SL**, a single-level joint encoder-decoder adaptation of contrastive dense SSL frameworks. We show that jointly pre-training the encoder with a decoder enhances the representation power of the encoder and improves downstream dense prediction performance, even without transferring the pre-trained decoder.

- We improve on this adaptation by introducing **DeCon-ML**, which extends DeCon-SL with a multi-level decoder loss function and an encoder level-wise channel dropout to promote a comprehensive feature usage of the encoder. It achieves state-of-the-art results on COCO object detection and instance segmentation and matches top performance on Pascal VOC semantic segmentation.
- We demonstrate that DeCon improves the encoder’s downstream performance compared to encoder-only frameworks, even when pre-training and fine-tuning decoders differ.
- We show that DeCon’s efficiency persists in out-of-domain downstream tasks and provides even greater benefits in scenarios with limited annotated fine-tuning data.

2. Related works

Self-Supervised pre-training: In SSL, deep learning models are trained on pretext tasks where the data itself provides supervision, which allow models to learn meaningful representations without any manual annotations. Early SSL works focused on designing these tasks, such as predicting missing parts of an image (image inpainting) [38], context prediction [16], solving jigsaw puzzles [34], coloring grayscale images [52], and predicting rotations [20]. These methods aimed to create surrogate objectives that encourage models to develop feature representations, which could later be transferred to downstream tasks. However, these methods often produced task-specific representations with limited generalizability and restricted scalability.

Recent methods prioritize generalizability and move away from hand-crafted pretext tasks. These approaches can be broadly categorized into generative and contrastive methods. Generative approaches in SSL aim to learn meaningful representations by modeling the underlying data distribution. This is typically achieved through reconstruction-based methods, where the model predicts corrupted parts of the input [1, 17, 23, 51], or adversarial methods, where a generative model learns to synthesize realistic samples while an encoder captures high-level features [26, 48]. Contrastive methods, which are the focus of this research, learn data representations by maximizing the similarity between features extracted from two augmented views of the same image. To avoid model collapse—a phenomenon where the model maps all inputs to the same representation—negative pairs [8, 22], stop-gradient mechanisms [9], variance regularization [2, 3], momentum contrast [22] or other architectural and optimization techniques are employed [5].

Dense pre-training: Even though most of the aforementioned frameworks can be used for downstream segmentation or detection, these models are not designed specifically for pixel-level, i.e., dense downstream tasks. Consequently, developing SSL approaches that generalize well to dense

downstream tasks, such as the segmentation task, is an active area of research [3, 35, 44–46]. The main idea behind these approaches is to shift from a global image similarity to a local similarity. Local similarity can be enforced based on the location of pixels in an image [35, 44, 50], local pixel features [45], or both [3, 29, 37]. Local similarity can also be enforced in a region-based manner [19, 24, 46, 49]. These methods outperform those based solely on image-level global similarity in downstream dense tasks.

Encoder-Decoder pre-training: Encoder-decoder architectures with skip connections between the encoder and decoder layers (e.g., U-Net-like models) have achieved state-of-the-art results in many segmentation tasks [27, 40, 53]. A common approach for pre-training such models in a self-supervised manner is image reconstruction [4, 6, 30]. However, the presence of skip connections allows a substantial amount of information to bypass the encoder’s final layer—often referred to as the bottleneck layer—resulting in lower-quality embeddings generated by the encoder. Our proposed approach preserves skip connections while addressing the issue of inferior representations generated by the decoder. Encoder-only contrastive learning frameworks are built solely around an encoder, incorporating components such as predictors and projectors. However, they do not include a decoder, even though a randomly initialized decoder is later attached to the pre-trained encoder in downstream dense tasks to form a complete architecture. While some generative SSL frameworks use a decoder for pre-training [14, 23, 38], to the best of our knowledge, no work has explored pre-training vision models with both encoder and decoder loss in a contrastive learning framework to learn a data representation.

3. Methods

We introduce two architectural adaptations, as depicted in Fig. 1: (A) a single-level decoder loss (DeCon-SL) and (B) a multi-level decoder loss (DeCon-ML).

3.1. DeCon-SL

Given a vision SSL framework that pre-trains an encoder using a teacher-student architecture [25], we retain the encoders and any existing “auxiliary layers” (e.g., predictors, projection heads), and add decoders and their corresponding auxiliary layers for both teacher and student networks. For all models, the auxiliary layers are designed to match those of the encoder, with adjustments applied to align with the decoder’s output feature size. We obtain two losses, one is computed from the encoder features while the other one is computed from the decoder features. Consequently, the loss function is defined as follows:

$$Loss = \alpha \times L_{enc} + (1 - \alpha) \times L_{dec} \quad (1)$$

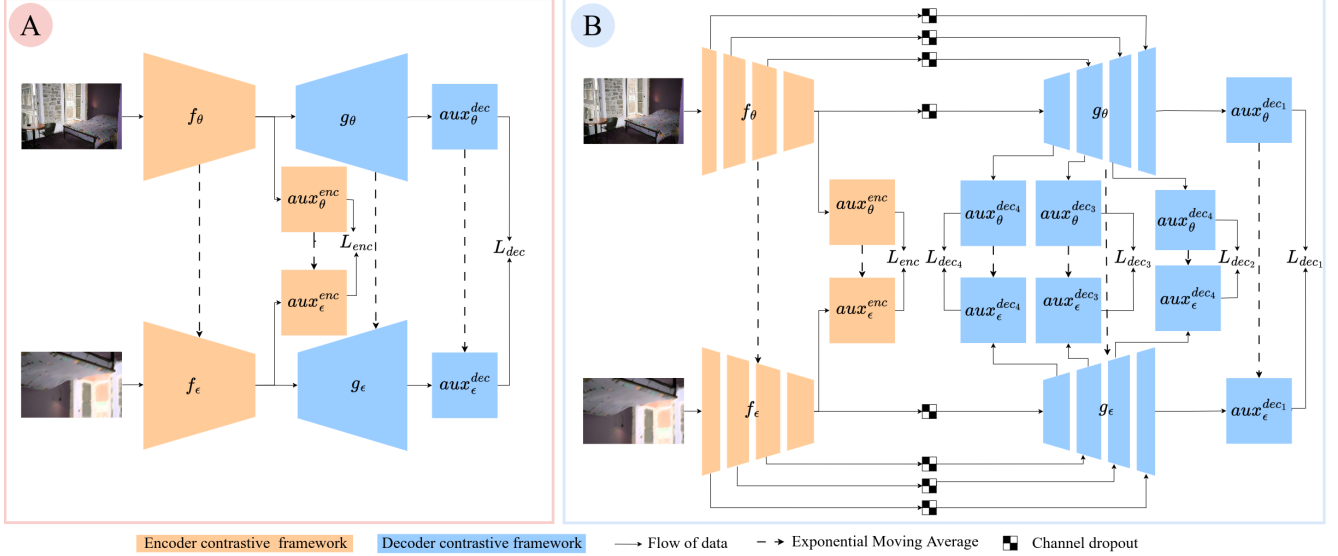


Figure 1. **A: DeCon-SL.** Instead of a classical encoder-only pre-training, a decoder is pre-trained alongside the encoder. We mirror the encoder loss at the decoder level and optimize the architecture using a weighted sum of the encoder and decoder losses. **B: DeCon-ML.** Instead of computing the decoder loss at a single level, it is calculated across multiple levels (four in this figure). Additionally, a channel-wise dropout is applied at the output of each encoder level before it is passed through the skip connection to the decoder.

where, α represents the contribution of the encoder loss in the objective function.

The DeCon-SL architecture is illustrated in Fig. 1 A, where f_θ and f_ϵ represent teacher and student encoders, respectively. aux_θ^{enc} and aux_ϵ^{enc} are the SSL framework’s auxiliary layers of the teacher and student encoders, respectively. Auxiliary layers can include any projector, predictor heads, or any layers used in the loss definition of the original SSL framework. g_θ and g_ϵ are the decoders of the teacher and student networks, and aux_θ^{dec} and aux_ϵ^{dec} are the auxiliary layers feeding from their respective decoder. g_θ and g_ϵ take the output of encoder f_θ and f_ϵ as input, respectively. Auxiliary layers aux_θ^{enc} and aux_ϵ^{enc} are responsible for generating a representation from the encoder output, that is used to compute a contrastive loss for the encoders $L^{encoder}$. The contrastive loss, $L^{decoder}$ is calculated from the representation obtained from the auxiliary layers of the decoders, i.e., aux_θ^{dec} and aux_ϵ^{dec} . f_ϵ and g_ϵ are updated using the exponential moving average (EMA) of f_θ and g_θ , respectively.

3.2. DeCon-ML

To address the challenge posed by skip connections between the encoder and decoder layers (as mentioned in the Related works section), we introduce a multi-layer contrastive decoder loss, consisting of a single loss for the encoder and multiple loss components for the decoder along with channel dropout and deep supervision, which we describe in detail below. Figure 1 B illustrates the DeCon-ML adaptation of a given SSL framework.

Channel dropout: The dropout layer is typically used to prevent overfitting, improve generalization, and act as an implicit ensemble [41, 43]. However, we extend its use by applying dropout to channels transferred through skip connections between the encoder and decoder. This prevents the model from relying heavily on specific features shared through skip connections and enforces full encoder training, leading to richer data representations at the bottleneck layer of the encoder. In DeCon-ML, we apply channel dropout to the output layers of the encoder at the different levels when passing these outputs to the decoder. No channel is zeroed-out when the inputs pass through the encoder. This channel dropout promotes a more comprehensive utilization of the encoder parameters and enhances representation power at various encoder levels while preserving the input information content as it passes through the encoder to its bottleneck.

Decoder deep supervision: An encoder-decoder SSL framework allows us to retrieve meaningful features from multiple levels of the decoder. We can then pre-train the architecture with multiple losses using decoder deep supervision. If the decoder is connected to the encoder at multiple levels through lateral/skip connections, decoder deep supervision strengthens the representation power of the encoder at different levels [39]. Since a decoder passes the encoder bottleneck representation in a bottom-up manner to its upper level layers, the final encoder bottleneck representation remains a non-negligible objective of the training since it impacts all decoder level losses. In contrast, applying deep supervision at multiple encoder stages in an encoder-

only SSL framework might prevent the creation of a strong semantic representation at the encoder bottleneck. To perform the decoder deep supervision, we add auxiliary layers to each decoder level, and a loss is computed at each level between the teacher and student representations. When performing decoder deep supervision, the encoder loss will remain the same as Eq. (1), but the decoder loss will be updated as follows:

$$Loss = \alpha \times L_{enc} + (1 - \alpha) \times L_{dds} \quad (2)$$

$$L_{dds} = \frac{1}{j} \times \sum_{i=1}^j L_{dec_i} \quad (3)$$

where j is the number of decoder levels at which a loss will be calculated and L_{dec_i} is the loss computed at level i . The final decoder loss in Eq. (2) is thus an average of the losses at the different levels.

3.3. Implementation details

Architecture: Following common practice in contrastive SSL approaches literature, we use a ResNet-50 encoder [21] as a backbone, a Feature Pyramid Network (FPN) [32] for downstream detection and instance segmentation, and a Fully Convolutional Network (FCN) [33] for downstream semantic segmentation [22, 45, 46] tasks. We implement FCN and skip-connected FPN as two decoder architectures in the DeCon framework adaptation. We follow the *mmseg* [11] FCN implementation used in SlotCon [46] and customize FPN implementation from *Detectron2* [47] version 0.6. We use DeCon to adapt the SlotCon [46] and DenseCL [45] frameworks. More implementation details are available in Supplementary Material Section 1.

For SlotCon, the student and teacher encoders, and every auxiliary layers—i.e., the respective projectors and semantic groupings, the slot predictor and the prototypes—are kept unchanged. Two decoders, a student and a teacher decoder (either FCN or FPN), that take the output of their corresponding encoder as input are added to the framework. The auxiliary layers are replicated at the decoder level. In the case of decoder deep supervision with FPN decoders, auxiliary layers are replicated independently at the four decoder levels. No deep supervision is performed in the DeCon adaptation of SlotCon with an FCN decoder. The decoder projectors differ from the encoder projectors only in input channels: 2048 for the encoder and 256 for the FPN and FCN decoders. We follow SlotCon by updating the teacher branch and the encoder and decoder slot predictors with Backpropagation, the student branch with an EMA of the first one, and the prototypes centers with an EMA of the previous batch centers seen during training. Our implementation is based on the official SlotCon repository. Detailed figures of SlotCon DeCon-SL and DeCon-ML adaptations are available in the Supplementary Material Section 1.

For DenseCL, the two encoders, along with their respective auxiliary layers—i.e., the global and dense projection heads—are kept the same as well as the independent dictionaries for global and dense losses. Additionally, we introduce two decoders, which take their respective encoders’ outputs as inputs. We also replicate the encoder’s dense and global projection heads and dictionaries separately for the two decoders. As for SlotCon, the input dimension of the decoder projectors is 256 instead of 2048 for the encoder. The encoders and decoders dictionaries size is set to 16384. We follow DenseCL by updating the first branch of the architecture through Backpropagation, while the second branch is updated using an EMA of the first one. Due to extensive memory requirements of replicating dictionaries at each decoder level, we do not conduct decoder deep supervision or channel dropout (DeCon-ML) experiments with DenseCL. We adapt DenseCL implementation from *mmselfsup* package [12] version 1.0.0.

Pre-training setup: We pre-train DeCon on COCO 2017 dataset [31]. The augmentations and all the hyperparameters—learning rate, weight decay, schedulers, batch size, input shape, number of epochs, momentum, and so on—are kept the same as used in the original SSL framework: SlotCon or DenseCL. The SlotCon models are pre-trained for 800 epochs using a LARS optimizer, with a total batch size of 512 across all available GPUs. The base learning rate is 1.0 scaled with the batch size and updated with a cosine learning rate decay schedule using weight decay of 10^{-5} and a warm-up period of 5 epochs. The pre-trainings using FPN decoders are done using eight NVIDIA H100 GPUs (80GB each). The pre-trainings without decoder and with FCN decoders are conducted on one 80GB NVIDIA A100 GPU. The DenseCL models are pre-trained for 800 epochs using an SGD optimizer with a total batch size of 256. The base learning rate is 0.3 and is updated using a cosine learning rate decay schedule (0.0001 weight decay, 0.9 momentum). The pre-training experiments are conducted with eight NVIDIA A100 GPUs (40GB each).

To assess the DeCon framework on non scene-centric data, we pre-train SlotCon and a DeCon-SL adaptation of SlotCon with an FCN decoder on two small-scale datasets: ISIC 2017 and REFUGE described in Sec. 3.4. For ISIC dataset, we pre-train for 800 epochs with a batch size of 256 and a base learning rate of 1.0 linearly scaled with batch size. For REFUGE, we pre-train for 2400 epochs with a batch size of 192 and the same learning rate as for ISIC. These pre-trainings are performed with one NVIDIA A6000 GPU with 48GB of memory.

3.4. Evaluation protocol

We evaluate the different pre-trained models on object detection, semantic segmentation, and instance segmentation as downstream tasks. We either transfer the pre-trained en-

coder or both the encoder and decoder for each fine-tuning experiment. All fine-tuning results reported in this paper are averaged over three independent runs. The pre-trainings, however, are only run once. All fine-tuning experiments related to the same dataset are run on a similar platform with the same hardware. We perform object detection and instance segmentation using *Detectron2* package [47] version 0.6, whereas *mmsegmentation* [11] version 0.30.0 is used for semantic segmentation tasks.

Object detection and instance segmentation: We perform object detection on Pascal VOC dataset [18] and object detection and instance segmentation on COCO dataset [31]. We fine-tune a Faster R-CNN with a FPN C4 backbone using VOC *trainval07+12* dataset for 24000 iterations and evaluate on the VOC *test2007* set following previous works [22, 50]. For COCO object detection and instance segmentation, we fine-tune a Mask R-CNN with FPN backbone on the COCO *train2017* dataset with 90000 iterations and evaluate on COCO *val2017* split following SlotCon [46]. We initialize the network either with a pre-trained ResNet-50 encoder or with both a ResNet-50 encoder and a pre-trained FPN decoder, and fine-tune end-to-end in all cases. All the aforementioned experiments are performed using one NVIDIA A100 GPU with 80GB memory.

Semantic segmentation on in-domain datasets: We perform semantic segmentation on Pascal VOC [18] and Cityscapes [13] datasets that contain scene-centric data following SlotCon [46] and PixCon [37]. A ResNet-50 encoder with a two-layer FCN decoder, similar to the FCN decoder used during pre-training, is used. For Pascal VOC, we train on VOC *train.aug2012* set for 30000 iterations with a batch size of 16 and evaluate on VOC *val2012* set. For Cityscapes, we fine tune on the *train.fine* set for 90000 iterations with a batch size of 16 and evaluate on the *val.fine* set. We initialize the network either with a pre-trained ResNet-50 encoder or with both the ResNet-50 encoder and the FCN decoder pre-trained and fine-tune end-to-end in all cases. All the aforementioned experiments are performed using one NVIDIA A100 GPU with 80GB (Cityscapes) or 40GB (Pascal VOC) memory.

Semantic segmentation on out-of-domain datasets: We also evaluate generalizability to out-of-domain datasets for downstream tasks on different dataset sizes, considering 5, 25, and 100% randomly selected training samples. We fine-tune a ResNet-50 encoder coupled with an FCN decoder for semantic segmentation on REFUGE [36] and ISIC 2017 [10] dataset. REFUGE dataset contains 1200 retinal images in total representing 3 different classes: optic disk, optic cup, and background, divided into 400 training, 400 validation, and 400 testing samples. We train the ResNet-50-FCN network end-to-end for 80000 iterations with a batch size of 16 on the *training* set using one NVIDIA A100 GPU (40GB). The learning rate starts at 0.01 and decreases

with a polynomial scheduler with a power of 0.9. We evaluate the model on the *test* set using the last iteration checkpoint and report the results.

ISIC 2017 is a skin-lesion segmentation dataset which consists of 2000 training, 150 validation, and 600 testing images. We fine-tune the same ResNet-50-FCN architecture on the *training* set for 24000 iterations on one NVIDIA V100 with 32GB of memory. Hyper parameters are the same as for REFUGE. We evaluate on the *validation* set every 500 iterations, select the best checkpoint and report the results of this checkpoint on the *test* set.

4. Results

DeCon-SL: Table 1 shows the results of DeCon-SL adaptation. DeCon pre-trained components outperformed baseline models in downstream object detection and segmentation when only the encoder was transferred, except for Cityscapes semantic segmentation with SlotCon. The transfer of both a pre-trained encoder and an FCN decoder always improved the performance further compared to transferring the pre-trained encoder only. Transferring the encoder and the FPN decoder pre-trained with DeCon-SL adaptation of DenseCL did not always result in improving model performance for downstream tasks.

DeCon-ML: Table 2 shows the results of DeCon-ML adaptation. We can see that adding the decoder deep supervision and a channel dropout probability of 0.5 during pre-training always enhanced fine-tuning performance compared to baseline approach (SlotCon) and DeCon-SL adaptation in all object detection and instance segmentation tasks.

Impact of the channel dropout: Impact of channel dropout is highlighted in Tab. 3. The decoder deep supervision on its own did not always improve downstream performance when only transferring the encoder in DeCon-ML. When transferring both encoder and decoder, downstream performance improved on Pascal VOC but not on COCO, which was the dataset used for pre-training. When the decoder deep supervision was coupled with channel dropout, performance improved compared to DeCon-SL. The channel dropout probability impacted the downstream performance differently when transferring only the encoder or both encoder and decoder. A channel dropout probability of 0.5 led to the best performance when transferring the encoder only. When transferring both encoder and decoder, a lower channel dropout probability of 0.25 led to the best performance on Pascal VOC object detection, and COCO instance segmentation. Comparing the performance of DeCon-ML adaptation with an encoder-only pre-training, we observed improvements in all scenarios regardless of dropout values.

Impact of encoder loss weight in DeCon: As shown in Tab. 4, the encoder loss weight α played a crucial role

Table 1. Performance of DeCon-SL adaptation ($\alpha = 0.5$) of SlotCon and DenseCL using FPN and FCN as options for decoders as well as baseline approaches. COCO dataset was used for pre-training. The same decoder architecture was used for pre-training and fine-tuning. The architecture was then fine-tuned on various segmentation and object detection tasks. All fine-tuning results were averaged over three runs. Up and down arrows indicate better and worst performance compared to baseline, respectively.

Framework	Adaptation	Decoder	Loss		Transfer		Object Detection VOC			Object Detection COCO			Instance Seg. COCO		Semantic Seg. VOC City		
			L_{enc}	L_{dec}	enc	dec	AP	AP ₅₀	AP ₇₅	AP	AP ₅₀	AP ₇₅	AP	AP ₅₀	AP ₇₅	mIoU	mIoU
SlotCon	None	None	✓	✗	✓	✗	55.16	81.76	61.23	40.81	60.95	44.37	36.80	57.98	39.54	71.50	75.95
	DeCon-SL	FPN	✓	✓	✓	✗	55.57 ↑	81.75 ↓	61.76 ↑	40.94 ↑	60.97 ↑	44.82 ↑	36.92 ↑	58.03 ↑	39.80 ↑	-	-
		FCN	✓	✓	✓	✗	-	-	-	-	-	-	-	-	-	-	72.42 ↑
DenseCL	None	None	✓	✗	✓	✗	54.50	80.47	59.97	39.60	59.30	43.29	35.65	56.49	38.25	71.11	75.87
	DeCon-SL	FPN	✓	✓	✓	✗	54.71 ↑	80.65 ↑	60.44 ↑	39.60	59.36 ↑	43.31 ↑	35.74 ↑	56.45 ↓	38.40 ↑	-	-
		FCN	✓	✓	✓	✗	-	-	-	-	-	-	-	-	-	-	71.31 ↑

Table 2. Performance of DeCon-ML adaptation of SlotCon with $\alpha = 0.5$ and $dropout = 0.5$ pre-trained on COCO dataset. We used an FPN as a DeCon decoder during pre-training and fine-tuning. We averaged all fine-tuning results over three runs. Arrows indicate performance gain or loss compared to baseline.

Frame work	Adaptation	Loss			Transfer		Object Detection VOC			Object Detection COCO			Instance Segmentation COCO		
		L_{enc}	L_{dec}	L_{dds}	enc	dec	AP	AP ₅₀	AP ₇₅	AP	AP ₅₀	AP ₇₅	AP	AP ₅₀	AP ₇₅
SlotCon	None	✓	✗	✗	✓	✗	55.16	81.76	61.23	40.81	60.95	44.37	36.80	57.98	39.54
	DeCon-SL	✓	✓	✗	✓	✗	55.57 ↑	81.75 ↓	61.76 ↑	40.94 ↑	60.97 ↑	44.82 ↑	36.92 ↑	58.03 ↑	39.80 ↑
		✓	✓	✗	✓	✗	55.40 ↑	81.48 ↓	61.21 ↓	41.05 ↑	61.34 ↑	44.85 ↑	37.03 ↑	58.33 ↑	39.86 ↑
DeCon-ML	✓	✗	✓	✓	✓	✗	55.60 ↑	81.84 ↑	61.83 ↑	41.10 ↑	61.37 ↑	45.01 ↑	37.05 ↑	58.46 ↑	39.87 ↑
	✓	✗	✓	✓	✓	✗	55.57 ↑	81.77 ↑	61.76 ↑	41.15 ↑	61.38 ↑	44.89 ↑	37.05 ↑	58.43 ↑	39.88 ↑

in downstream performance. Decreasing α down to 0 for DeCon-ML pre-training and down to 0.25 for DeCon-SL pre-training increased the fine-tuning performance. This pattern was also observed when transferring both the encoder and the decoder. The downstream performance of DeCon adaptation was higher than that of encoder-only pre-training (baseline, $\alpha = 1$) for object detection and instance segmentation tasks, whether transferring only the encoder or both the encoder and decoder. For Cityscapes semantic segmentation, no pattern was observed regarding the relationship between the value of α and model performance.

Heterogeneous pre-training and fine-tuning decoders:

All the previous fine-tuning results were obtained using the pre-trained encoder of a DeCon adaptation, where the pre-training decoder matched the fine-tuning decoder. However, Tab. 5 shows that even if we pre-trained a DeCon adaptation of SlotCon with an FCN decoder and transferred the encoder only for an FPN-based downstream task, we obtained better performance than a baseline SlotCon pre-training. It is also true for the opposite scenario, when FPN decoder was used for pre-training DeCon-ML, and FCN decoder was used for fine-tuning.

Comparison with state-of-the-art: Table 6 shows that our top-performing DeCon-ML and DeCon-SL adaptations achieved better performance than state-of-the-art methods on COCO object detection and instance segmentation, and

VOC semantic segmentation tasks. A more detailed comparison is available in Supplementary Material Section 2.

DeCon-SL performance in out-of-domain tasks: Table 7 depicts the performance of a model pre-trained on COCO to out-of-domain datasets. We observed a consistent improvement of the DeCon-SL pre-training adaptation compared to the encoder-only pre-training for both REFUGE and ISIC; moreover, this gain increased when the dataset size decreased. Further improvement was achieved when transferring the pre-trained decoder along with the encoder for ISIC dataset. Additionally, pre-training only on ISIC dataset consistently resulted in better performance compared to pre-training on COCO dataset. However, pre-training on REFUGE dataset did not outperform COCO pre-trained approaches, potentially due to the lack of available images (only 400) to develop a strong enough representation during pre-training. In both cases, DeCon-SL pre-training adaptation outperformed encoder-only pre-training, even if we transferred only the encoder. We also observed that pre-trained models outperformed models trained with randomly initialized weights. This gap was more notable in REFUGE dataset (over 20%).

5. Discussion

In this paper, we introduced a contrastive framework adaptation by incorporating a decoder contrastive loss to an

Table 3. Impact of channel dropout probability on DeCon-ML. We pre-trained a DeCon-ML adaptation of SlotCon framework on COCO dataset with different channel dropout probabilities. We used an FPN as a DeCon decoder during pre-training and fine-tuning. We averaged all fine-tuning results over three runs.

Transfer	SSL	Loss			α	Dropout	VOC Object Detection			COCO Object Detection			COCO Instance Seg.		
		L_{enc}	L_{dec}	L_{dds}			AP	AP ₅₀	AP ₇₅	AP	AP ₅₀	AP ₇₅	AP	AP ₅₀	AP ₇₅
Enc	SlotCon	✓	✗	✗	1	0	55.16	81.76	61.23	40.81	60.95	44.37	36.80	57.98	39.54
	DeCon-SL	✓	✓	✗	0.5	0	55.57	81.75	61.76	40.94	60.97	44.82	36.92	58.03	39.80
		✓	✓	✗		0.5	55.20	81.56	61.33	40.90	61.23	44.64	36.91	58.30	39.67
	DeCon-ML	✓	✗	✓	0.5	0	55.52	81.67	62.01	40.85	60.95	44.67	36.83	58.12	39.55
		✓	✗	✓		0.25	55.54	81.88	61.10	40.95	61.13	44.88	36.97	58.22	39.76
		✓	✗	✓		0.5	55.60	81.84	61.83	41.10	61.37	45.01	37.05	58.46	39.87
✓	✗	✓	0.75	55.29	81.64	61.36	41.02	61.27	44.96	37.05	58.33	39.85			
Enc + Dec	DeCon-SL	✓	✓	✗	0.5	0	55.40	81.48	61.21	41.05	61.34	44.85	37.03	58.33	39.86
	DeCon-ML	✓	✗	✓		0	55.70	81.89	61.69	40.97	61.37	44.66	37.08	58.45	39.88
		✓	✗	✓	0.25	55.79	81.79	61.93	41.06	61.36	44.99	37.13	58.52	39.86	
		✓	✗	✓	0.5	55.57	81.77	61.76	41.15	61.38	44.89	37.05	58.43	39.88	
		✓	✗	✓	0.75	55.37	81.57	61.48	41.11	61.45	44.91	37.13	58.55	39.99	

Table 4. Impact of the encoder weight α . We pre-trained a DeCon-ML adaptation of SlotCon with an FPN decoder ($dropout = 0.5$) and a DeCon-SL adaptation of SlotCon with an FCN decoder on COCO dataset. We averaged all fine-tuning results over three runs.

Transfer	α	SSL strategy	Object Detection VOC			Object Detection COCO			Instance Seg. COCO			SSL strategy	Semantic Seg. VOC City	
			AP	AP ₅₀	AP ₇₅	AP	AP ₅₀	AP ₇₅	AP	AP ₅₀	AP ₇₅		mIoU	mIoU
Enc	1	SlotCon	55.16	81.76	61.23	40.81	60.95	44.37	36.80	57.98	39.54	SlotCon	71.50	75.95
	0.75	DeCon-ML-FPN 0.5 Dropout ($L_{enc} + L_{dds}$)	55.33	81.68	61.34	40.98	61.28	44.76	36.95	58.34	39.72	DeCon-SL-FCN ($L_{enc} + L_{ds}$)	71.98	76.18
	0.5		55.60	81.84	61.83	41.10	61.37	45.01	37.05	58.46	39.87		72.42	75.62
	0.25		55.69	81.98	62.05	41.05	61.19	44.85	37.08	58.29	39.70		73.01	76.21
	0		55.70	81.91	62.07	41.18	61.38	44.91	37.12	58.35	39.94		72.17	75.71
0.75	55.46		81.51	61.35	40.96	61.10	44.87	36.90	58.07	39.73	72.80		76.06	
Enc + Dec	0.5	55.57	81.77	61.76	41.15	61.38	44.89	37.05	58.43	39.88	72.58	75.97		
	0.25	55.67	81.91	61.62	41.17	61.41	44.87	37.13	58.46	39.76	72.96	76.28		
	0	55.61	81.83	61.60	41.21	61.39	44.99	37.11	58.41	39.92	71.61	75.38		

Table 5. Heterogeneous pre-training and fine-tuning decoders. We pre-trained a DeCon-SL adaptation of SlotCon with an FCN decoder and transferred the pre-trained encoder to FPN-based models for downstream tasks. Similarly, we pre-trained a DeCon-ML adaptation of SlotCon with an FPN decoder and transferred the pre-trained encoder to FCN-based models for downstream tasks. We averaged fine-tuning results over three runs.

Pretraining	α	Drop	Loss			Obj. Det. VOC	Obj. Det. COCO	Inst. Seg. COCO	Semantic Seg. VOC	Semantic Seg. City
			L_{enc}	L_{dec}	L_{dds}	AP	AP	AP	mIoU	mIoU
SlotCon	1	0	✓	✗	✗	55.16	40.81	36.80	71.50	75.95
DeCon-ML-FPN	0	0.5	✗	✓	✓	-	-	-	72.92	76.45
DeCon-SL-FCN	0.5	0	✓	✓	✗	55.29	40.96	36.98	-	-

existing framework. We showed that our proposed SSL adaptation outperforms previous state-of-the-art methods on COCO object detection and instance segmentation and achieves comparable results on Pascal VOC semantic segmentation (Tab. 6). This adaptation enhances the representation of the pre-trained encoder, improving its transfer performance for dense downstream tasks, regardless of the homogeneity between pre-training and fine-tuning decoders (as shown in Tab. 5). We showed that pre-training an FPN DeCon adaptation of SlotCon leads to better results when using deep supervision (DeCon-ML) compared to the base-

Table 6. Performance comparison with state-of-the-art models pre-trained on COCO. We only transferred the encoder for downstream tasks. We averaged fine-tuning results over three runs. †: Collected from PixCon paper. ‡: Full re-implementation. We picked the best performing DeCon-ML-FPN ($\alpha = 0$, $dropout = 0.5$) and DeCon-SL-FCN ($\alpha = 0.25$) adaptation of SlotCon.

Method	Obj. Det.		Inst. Seg.	Semantic Seg.	
	VOC	COCO	COCO	VOC	City
	APb	APb	APm	mIoU	mIoU
SlotCon ‡ [46]	55.16	40.81	36.80	71.50	75.95
PixCon-SR † [37]	57.55	40.81	36.84	72.95	76.62
DeCon-ML-SlotCon-FPN [ours]	55.70	41.18	37.12	72.92	76.45
DeCon-SL-SlotCon-FCN [ours]	-	-	-	73.01	76.21

lines as well as DeCon-SL, both when transferring encoder only and when transferring encoder and decoder. Framework specific hyperparameter tuning of the auxiliary layers could increase further the performance, as shown in Supplementary material Section 3.

We introduced a combined loss where encoder and decoder loss contribute to the total loss in a weighted manner. We observed that increasing the weight for the decoder loss compared to that of the encoder enhances the performance of the pre-trained models on downstream tasks. This could be attributed to the non-competing nature of an en-

Table 7. Transfer performance on out-of-domain datasets using randomly initialized or pre-trained weights. We pre-trained SlotCon and its DeCon-SL adaptation with an FCN decoder ($\alpha = 0.5$) on COCO, REFUGE and ISIC training datasets. We fine-tuned on REFUGE and ISIC datasets under various dataset sizes. We averaged the fine-tuning mIoU results over three runs.

SSL strategy	Loss		Transfer		Pre-trained on COCO						Pre-trained on Downstream Data	
	L_{enc}	L_{dec}	enc	dec	Refuge			ISIC			Refuge	ISIC
					5%	25%	100%	5%	25%	100%		
Random init.	-	-	-	-	49.53	41.41	62.82	75.66	78.38	80.65	62.82	80.65
SlotCon	✓	✗	✓	✗	69.60	77.80	82.83	74.95	79.05	82.52	79.86	83.19
DeCon-SL	✓	✓	✓	✗	71.75	78.92	83.57	75.62	79.56	82.84	80.71	83.66
	✓	✓	✓	✓	72.09	77.27	83.25	76.00	79.97	82.94	81.01	83.25

coder and decoder loss compared to approaches that utilize a construction loss for a decoder and a different loss for the encoder in an encoder-decoder architecture [28]. Moreover, we noticed that the encoder loss is optional when pre-training with DeCon-ML, demonstrating the efficiency of the decoder deep supervision and channel dropout combination to ensure a comprehensive pre-training of both encoder and decoder. The lack of skip-connections in DeCon-SL with FCN decoder makes the combined encoder-decoder loss preferable to ensure the best pre-training. We also observed in Tab. 3 that dropout does not provide the same benefits in DeCon-SL compared to DeCon-ML. Hence, channel dropout should only be applied to the different encoder levels when pre-training with a skip-connected decoder and decoder deep supervision (DeCon-ML).

As shown in Tab. 1, DeCon-SL adaptation of an SSL framework also allows for pre-training a decoder efficiently. However, transferring the FPN decoder along the encoder for VOC object detection did not increase detection performance compared to transferring only the encoder, potentially indicating a form of over-fitting of the FPN decoder to the pre-training dataset. This is alleviated by deep supervision in DeCon-ML adaptation as shown in Tab. 3. We showed that DeCon can be used to adapt two different SSL frameworks using different concepts to learn local information (pixel level VS object/group level). This suggests that the proposed DeCon adaptation can be used in any SSL contrastive method designed for dense downstream tasks.

While DeCon-SL adaptation with an FCN decoder benefits DenseCL framework, the added value of the FPN decoder transfer in DeCon-SL adaptation of DenseCL was not obvious on object detection and instance segmentation downstream tasks. However, the added value of the FPN decoder transfer in DeCon-SL adaptation of SlotCon was present across all scenarios, enhancing model performance, possibly due to the region-based contrastive mechanism of SlotCon. We could not investigate the impact of DeCon-ML adaptation on DenseCL due to its extensive memory requirements, which can be attributed to its reliance on a large number of negative pairs.

DeCon’s performance on VOC object detection and Cityscapes semantic segmentation is constrained by its base SSL framework, SlotCon, preventing it from surpassing the state-of-the-art (PixCon) for these tasks (Tab. 6). As an adaptation, DeCon’s effectiveness largely depends on the underlying framework. While integrating DeCon with the latest state-of-the-art framework could set a new benchmark across all datasets, we were unable to implement PixCon due to the unavailability of its code [37].

DeCon adaptation of an SSL framework was also advantageous for fine-tuning on small scale datasets and out-of-domain dense tasks compared to the encoder-only baseline framework (see Tab. 7). This benefit was also observed when pre-training directly on the target dataset. In such cases, DeCon is valuable compared to an encoder-only pre-training whether we transfer the pre-trained decoder or not.

One limitation of our approach is its high memory and computational demand. Pre-training a decoder using DeCon can significantly increase the parameter count and training time, which can restrict this approach to certain SSL frameworks. For example, the DeCon-SL adaptation of SlotCon with FPN decoder could not fit in a single 80GB memory GPU. More details on the parameter count are available in Supplementary Material Section 4. Another limitation of our work is that we only considered ResNet-50 backbone; however, we expect achieving superior results when using more efficient backbones such as EfficientNet [42].

Brempong et al. [4] followed a staged approach, first pre-training the encoder with supervision on annotated datasets, then pre-training the decoder with denoising. However, this multi-stage process relies on labeled data. It could also result in suboptimal feature alignment and increased training complexity. Future works could involve extending our proposed SSL adaptation to offer a multi-stage continual pre-training in a contrastive manner.

6. Conclusion

In this paper, we introduced DeCon—a novel contrastive framework adaptation that enhances the performance of self-supervised learning approaches for dense predictions tasks, such as object detection, semantic segmentation, and instance segmentation. We showed that not-only does this adaptation provide a solution for pre-training decoders, but it also improves the encoder’s representation significantly. We proposed two variants of DeCon: DeCon-SL and DeCon-ML. The former introduces a decoder contrastive loss, and the latter extends DeCon-SL by introducing channel dropout and decoder deep supervision to maximize the encoder’s pre-training power. By integrating these enhancements into an existing framework, we demonstrated that DeCon outperforms or matches state-of-the-art methods across multiple downstream dense prediction tasks.

References

- [1] Mahmoud Assran, Quentin Duval, Ishan Misra, Piotr Bojanowski, Pascal Vincent, Michael Rabbat, Yann LeCun, and Nicolas Ballas. Self-supervised learning from images with a joint-embedding predictive architecture. In *2023 IEEE/CVF Conference on Computer Vision and Pattern Recognition (CVPR)*, pages 15619–15629, 2023. 2
- [2] Adrien Bardes, Jean Ponce, and Yann LeCun. Vicreg: Variance-invariance-covariance regularization for self-supervised learning. In *ICLR*, 2022. 1, 2
- [3] Adrien Bardes, Jean Ponce, and Yann LeCun. Vicregl: Self-supervised learning of local visual features. In *NeurIPS*, 2022. 2
- [4] Emmanuel Asiedu Brempong, Simon Kornblith, Ting Chen, Niki Parmar, Matthias Minderer, and Mohammad Norouzi. Denoising pretraining for semantic segmentation. In *Proceedings of the IEEE/CVF Conference on Computer Vision and Pattern Recognition (CVPR) Workshops*, pages 4175–4186, 2022. 2, 8
- [5] Mathilde Caron, Hugo Touvron, Ishan Misra, Hervé Jegou, Julien Mairal, Piotr Bojanowski, and Armand Joulin. Emerging properties in self-supervised vision transformers. In *2021 IEEE/CVF International Conference on Computer Vision (ICCV)*, pages 9630–9640, 2021. 2
- [6] Liang Chen, Paul Bentley, Kensaku Mori, Kazunari Misawa, Michitaka Fujiwara, and Daniel Rueckert. Self-supervised learning for medical image analysis using image context restoration. *Medical Image Analysis*, 58:101539, 2019. 2
- [7] Ting Chen, Simon Kornblith, Mohammad Norouzi, and Geoffrey Hinton. A simple framework for contrastive learning of visual representations. *arXiv preprint arXiv:2002.05709*, 2020. 1
- [8] Ting Chen, Simon Kornblith, Mohammad Norouzi, and Geoffrey Hinton. A simple framework for contrastive learning of visual representations. *arXiv preprint arXiv:2002.05709*, 2020. 2
- [9] Xinlei Chen and Kaiming He. Exploring simple siamese representation learning. In *Proceedings of the IEEE/CVF Conference on Computer Vision and Pattern Recognition (CVPR)*, pages 15750–15758, 2021. 2
- [10] Noel CF Codella, David Gutman, M Emre Celebi, Brian Helba, Michael A Marchetti, Stephen W Dusza, Aadi Kallou, Konstantinos Liopyris, Nabin Mishra, Harald Kittler, et al. Skin lesion analysis toward melanoma detection: A challenge at the 2017 international symposium on biomedical imaging (isbi), hosted by the international skin imaging collaboration (isic). In *2018 IEEE 15th international symposium on biomedical imaging (ISBI 2018)*, pages 168–172. IEEE, 2018. 5
- [11] MMSegmentation Contributors. MMSegmentation: Openmmlab semantic segmentation toolbox and benchmark. <https://github.com/open-mmlab/mms Segmentation>, 2020. 4, 5
- [12] MMSelfSup Contributors. MMSelfSup: Openmmlab self-supervised learning toolbox and benchmark. <https://github.com/open-mmlab/mmselfsup>, 2021. 4
- [13] Marius Cordts, Mohamed Omran, Sebastian Ramos, Timo Rehfeld, Markus Enzweiler, Rodrigo Benenson, Uwe Franke, Stefan Roth, and Bernt Schiele. The cityscapes dataset for semantic urban scene understanding. In *Proceedings of the IEEE conference on computer vision and pattern recognition*, pages 3213–3223, 2016. 5
- [14] Zhigang Dai, Bolun Cai, Yugeng Lin, and Junying Chen. Up-detr: Unsupervised pre-training for object detection with transformers. In *Proceedings of the IEEE/CVF Conference on Computer Vision and Pattern Recognition (CVPR)*, pages 1601–1610, 2021. 2
- [15] Jia Deng, Wei Dong, Richard Socher, Li-Jia Li, Kai Li, and Li Fei-Fei. Imagenet: A large-scale hierarchical image database. In *2009 IEEE Conference on Computer Vision and Pattern Recognition*, pages 248–255, 2009. 1
- [16] Carl Doersch, Abhinav Gupta, and Alexei A. Efros. Unsupervised visual representation learning by context prediction. In *Proceedings of the IEEE International Conference on Computer Vision (ICCV)*, 2015. 2
- [17] Xiaoyi Dong, Jianmin Bao, Ting Zhang, Dongdong Chen, Weiming Zhang, Lu Yuan, Dong Chen, Fang Wen, Nenghai Yu, and Baining Guo. PeCo: Perceptual Codebook for BERT Pre-training of Vision Transformers. *Proceedings of the AAAI Conference on Artificial Intelligence*, 37(1):552–560, 2023. 2
- [18] Mark Everingham, SM Ali Eslami, Luc Van Gool, Christopher KI Williams, John Winn, and Andrew Zisserman. The pascal visual object classes challenge: A retrospective. *International journal of computer vision*, 111:98–136, 2015. 5
- [19] Chongjian Ge, Jiangliu Wang, Zhan Tong, Shoufa Chen, Yibing Song, and Ping Luo. Soft neighbors are positive supporters in contrastive visual representation learning. *arXiv preprint arXiv:2303.17142*, 2023. 2
- [20] Spyros Gidaris, Praveer Singh, and Nikos Komodakis. Unsupervised representation learning by predicting image rotations. *arXiv preprint arXiv:1803.07728*, 2018. 2
- [21] Kaiming He, Xiangyu Zhang, Shaoqing Ren, and Jian Sun. Deep residual learning for image recognition. In *2016 IEEE Conference on Computer Vision and Pattern Recognition (CVPR)*, pages 770–778, 2016. 4
- [22] Kaiming He, Haoqi Fan, Yuxin Wu, Saining Xie, and Ross Girshick. Momentum contrast for unsupervised visual representation learning. In *2020 IEEE/CVF Conference on Computer Vision and Pattern Recognition (CVPR)*, pages 9726–9735, 2020. 1, 2, 4, 5
- [23] Kaiming He, Xinlei Chen, Saining Xie, Yanghao Li, Piotr Dollár, and Ross Girshick. Masked autoencoders are scalable vision learners. In *2022 IEEE/CVF Conference on Computer Vision and Pattern Recognition (CVPR)*, pages 15979–15988, 2022. 2
- [24] Olivier J Hénaff, Skanda Koppula, Evan Shelhamer, Daniel Zoran, Andrew Jaegle, Andrew Zisserman, João Carreira, and Relja Arandjelović. Object discovery and representation networks. In *European conference on computer vision*, pages 123–143. Springer, 2022. 2
- [25] Geoffrey Hinton, Oriol Vinyals, and Jeff Dean. Distilling the knowledge in a neural network, 2015. 2

- [26] Drew A. Hudson, Daniel Zoran, Mateusz Malinowski, Andrew K. Lampinen, Andrew Jaegle, James L. McClelland, Loic Matthey, Felix Hill, and Alexander Lerchner. Soda: Bottleneck diffusion models for representation learning. In *Proceedings of the IEEE/CVF Conference on Computer Vision and Pattern Recognition (CVPR)*, pages 23115–23127, 2024. 2
- [27] Fabian Isensee, Paul F. Jaeger, Simon A. A. Kohl, Jens Petersen, and Klaus H. Maier-Hein. nnU-Net: a self-configuring method for deep learning-based biomedical image segmentation. *Nature Methods*, 18(2):203–211, 2021. 2
- [28] Ziyu Jiang, Yinpeng Chen, Mengchen Liu, Dongdong Chen, Xiyang Dai, Lu Yuan, Zicheng Liu, and Zhangyang Wang. Layer Grafted Pre-training: Bridging Contrastive Learning And Masked Image Modeling For Label-Efficient Representations, 2023. arXiv:2302.14138. 8
- [29] Tim LeBailly and Tinne Tuytelaars. Global-local self-distillation for visual representation learning. In *2023 IEEE/CVF Winter Conference on Applications of Computer Vision (WACV)*, pages 1441–1450, 2023. 2
- [30] Junjie Liang, Cihui Yang, Jingting Zhong, and Xiaoli Ye. BTSwin-Unet: 3D U-shaped Symmetrical Swin Transformer-based Network for Brain Tumor Segmentation with Self-supervised Pre-training. *Neural Processing Letters*, 55(4):3695–3713, 2023. 2
- [31] Tsung-Yi Lin, Michael Maire, Serge Belongie, Lubomir Bourdev, Ross Girshick, James Hays, Pietro Perona, Deva Ramanan, C. Lawrence Zitnick, and Piotr Dollár. Microsoft COCO: Common Objects in Context, 2015. arXiv:1405.0312 [cs]. 4, 5
- [32] Tsung-Yi Lin, Piotr Dollár, Ross Girshick, Kaiming He, Bharath Hariharan, and Serge Belongie. Feature pyramid networks for object detection. In *Proceedings of the IEEE Conference on Computer Vision and Pattern Recognition (CVPR)*, 2017. 4
- [33] Jonathan Long, Evan Shelhamer, and Trevor Darrell. Fully convolutional networks for semantic segmentation. In *2015 IEEE Conference on Computer Vision and Pattern Recognition (CVPR)*, pages 3431–3440, Los Alamitos, CA, USA, 2015. IEEE Computer Society. 4
- [34] Mehdi Noroozi and Paolo Favaro. Unsupervised learning of visual representations by solving jigsaw puzzles. In *European conference on computer vision*, pages 69–84. Springer, 2016. 2
- [35] Pedro O O. Pinheiro, Amjad Almahairi, Ryan Benmalek, Florian Golemo, and Aaron C Courville. Unsupervised learning of dense visual representations. In *Advances in Neural Information Processing Systems*, pages 4489–4500. Curran Associates, Inc., 2020. 2
- [36] José Ignacio Orlando, Huazhu Fu, João Barbosa Breda, Karel Van Keer, Deepti R Bathula, Andrés Diaz-Pinto, Ruogu Fang, Pheng-Ann Heng, Jeyoung Kim, JoonHo Lee, et al. Refuge challenge: A unified framework for evaluating automated methods for glaucoma assessment from fundus photographs. *Medical image analysis*, 59:101570, 2020. 5
- [37] Zongshang Pang, Yuta Nakashima, Mayu Otani, and Hajime Nagahara. Revisiting pixel-level contrastive pre-training on scene images. In *Proceedings of the IEEE/CVF Winter Conference on Applications of Computer Vision (WACV)*, pages 1784–1793, 2024. 1, 2, 5, 7, 8
- [38] Deepak Pathak, Philipp Krähenbühl, Jeff Donahue, Trevor Darrell, and Alexei A. Efros. Context encoders: Feature learning by inpainting. In *2016 IEEE Conference on Computer Vision and Pattern Recognition (CVPR)*, pages 2536–2544, 2016. 2
- [39] Simon Reiss, Constantin Seibold, Alexander Freytag, Erik Rodner, and Rainer Stiefelhagen. Every annotation counts: Multi-label deep supervision for medical image segmentation. In *Proceedings of the IEEE/CVF Conference on Computer Vision and Pattern Recognition (CVPR)*, pages 9532–9542, 2021. 3
- [40] Olaf Ronneberger, Philipp Fischer, and Thomas Brox. U-net: Convolutional networks for biomedical image segmentation. In *Medical Image Computing and Computer-Assisted Intervention – MICCAI 2015*, pages 234–241, Cham, 2015. Springer International Publishing. 2
- [41] Nitish Srivastava, Geoffrey Hinton, Alex Krizhevsky, Ilya Sutskever, and Ruslan Salakhutdinov. Dropout: A simple way to prevent neural networks from overfitting. *Journal of Machine Learning Research*, 15(56):1929–1958, 2014. 3
- [42] Mingxing Tan and Quoc Le. EfficientNet: Rethinking model scaling for convolutional neural networks. In *Proceedings of the 36th International Conference on Machine Learning*, pages 6105–6114. PMLR, 2019. 8
- [43] Jonathan Tompson, Ross Goroshin, Arjun Jain, Yann LeCun, and Christoph Bregler. Efficient object localization using convolutional networks. In *2015 IEEE Conference on Computer Vision and Pattern Recognition (CVPR)*, pages 648–656, 2015. 3
- [44] Feng Wang, Huiyu Wang, Chen Wei, Alan Yuille, and Wei Shen. Cp 2: Copy-paste contrastive pretraining for semantic segmentation. In *European Conference on Computer Vision*, pages 499–515. Springer, 2022. 2
- [45] Xinlong Wang, Rufeng Zhang, Chunhua Shen, Tao Kong, and Lei Li. Dense contrastive learning for self-supervised visual pre-training. In *2021 IEEE/CVF Conference on Computer Vision and Pattern Recognition (CVPR)*, pages 3023–3032, 2021. 1, 2, 4
- [46] Xin Wen, Bingchen Zhao, Anlin Zheng, Xiangyu Zhang, and Xiaojuan Qi. Self-supervised visual representation learning with semantic grouping. In *Advances in Neural Information Processing Systems*, pages 16423–16438. Curran Associates, Inc., 2022. 2, 4, 5, 7
- [47] Yuxin Wu, Alexander Kirillov, Francisco Massa, Wan-Yen Lo, and Ross Girshick. Detectron2. <https://github.com/facebookresearch/detectron2>, 2019. 4, 5
- [48] Weilai Xiang, Hongyu Yang, Di Huang, and Yunhong Wang. Denoising diffusion autoencoders are unified self-supervised learners. In *Proceedings of the IEEE/CVF International Conference on Computer Vision (ICCV)*, pages 15802–15812, 2023. 2
- [49] Jiahao Xie, Xiaohang Zhan, Ziwei Liu, Yew Soon Ong, and Chen Change Loy. Unsupervised object-level representation

- learning from scene images. In *Advances in Neural Information Processing Systems*, pages 28864–28876. Curran Associates, Inc., 2021. [2](#)
- [50] Zhenda Xie, Yutong Lin, Zheng Zhang, Yue Cao, Stephen Lin, and Han Hu. Propagate yourself: Exploring pixel-level consistency for unsupervised visual representation learning. In *2021 IEEE/CVF Conference on Computer Vision and Pattern Recognition (CVPR)*, pages 16679–16688, 2021. [2](#), [5](#)
- [51] Zhenda Xie, Zheng Zhang, Yue Cao, Yutong Lin, Jianmin Bao, Zhuliang Yao, Qi Dai, and Han Hu. Simmim: A simple framework for masked image modeling. In *Proceedings of the IEEE/CVF Conference on Computer Vision and Pattern Recognition (CVPR)*, pages 9653–9663, 2022. [2](#)
- [52] Richard Zhang, Phillip Isola, and Alexei A. Efros. Colorful image colorization. In *Computer Vision – ECCV 2016*, pages 649–666, Cham, 2016. Springer International Publishing. [2](#)
- [53] Zongwei Zhou, Md Mahfuzur Rahman Siddiquee, Nima Tajbakhsh, and Jianming Liang. UNet++: A Nested U-Net Architecture for Medical Image Segmentation. In *Deep Learning in Medical Image Analysis and Multimodal Learning for Clinical Decision Support*, pages 3–11, Cham, 2018. Springer International Publishing. [2](#)

Supplementary Materials: Should we pre-train a decoder in contrastive learning for dense prediction tasks?

1. Framework specifics

Figure 1 presents the DeCon-SL-adaptation of SlotCon SSL framework to an encoder-decoder framework. Figure 2 illustrates how we used channel dropout and decoder deep-supervision for the DeCon-ML adaptation of SlotCon framework with FPN decoder pre-training.

1.1. Fully Convolutional Network

To match previous evaluation with mmseg framework, we implement a fully convolutional Network (FCN) as a two 3×3 convolutional block of 256 channels (dilation set to 6) with batch normalization and ReLU activations.

1.2. Feature Pyramid Network

Feature Pyramid Network (FPN) C5 implementation is customized from the Detectron2 library. The architecture has four lateral convolutional layers. Each layer uses a 1×1 convolution to reduce the ResNet-50 outputs from 2048, 1024, 512, and 256 channels down to 256 channels. We then sum these lateral outputs in a bottom-up manner and pass the combined output through a 3×3 convolution to produce a 256-channel decoder output. For deep supervision, we apply a 3×3 convolution at each of the four levels. These four decoder outputs are passed as input to four different auxiliary layers to provide four decoder losses. Note that, deep supervision loss is only calculated in FPN scenario where lateral connections are present.

2. Performance comparison with state of the art methods

Table 1 demonstrated performance comparison between our best approaches DeCon-ML-Slotcon-FPN ($\alpha = 0$, $dropout = 0.5$) and DeCon-SL-FCN ($\alpha = 0.25$) adaptation of SlotCon with state-of-the-art methods. We achieved the state-of-the performance on COCO object detection and COCO instance segmentation. Our results are on par with state-of-the-art methods on Pascal VOC semantic segmentation.

3. Improving DeCon performance with decoder-specific hyperparameter tuning

Hyperparameters used in the “auxiliary layers” of the encoder were replicated at the decoder level. Table 2 shows that tuning these hyperparameters for the decoder could result in better downstream performance. 384 prototypes used in the decoder loss computation results in better downstream performance than the encoder’s parameter: 256 prototypes, taken from the original SlotCon framework.

4. Pre-training parameter counts

Parameter counts in encoder, decoder, auxiliary layers, GPU setup and time per epoch to train the models are provided in Tab. 3. DeCon parameter count is higher mostly due to auxiliary layers which is not used for fine-tuning.

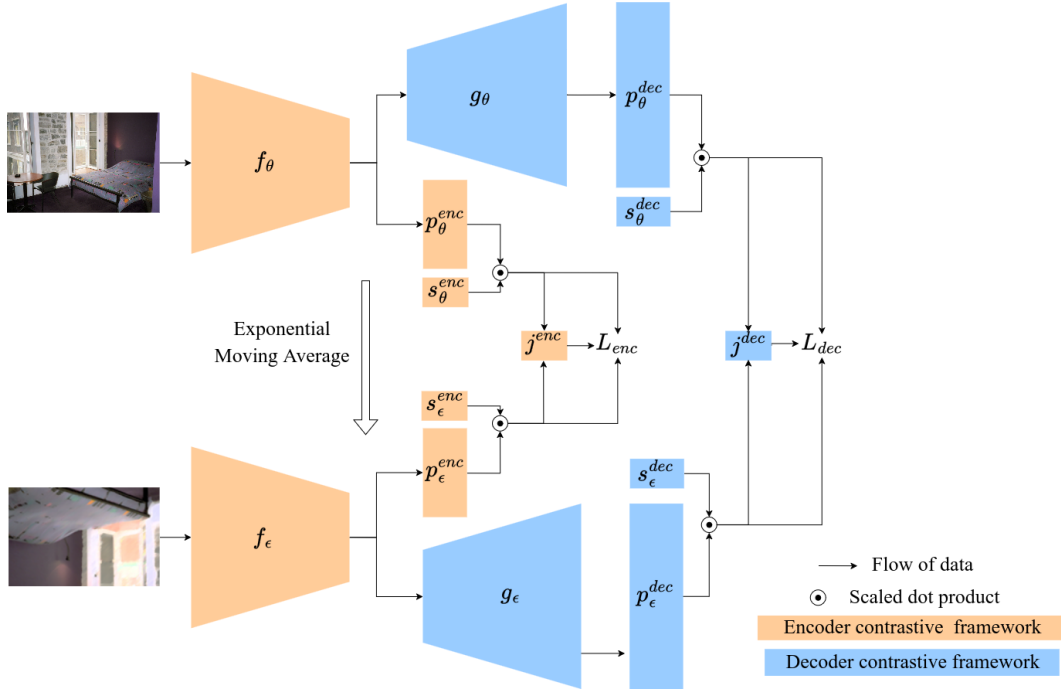


Figure 1. This figure illustrates the proposed DeCon-SL adaptation of SlotCon framework with an FCN decoder. f_θ and f_ϵ represent teacher and student encoders, respectively. p_θ^{enc} and p_ϵ^{enc} are the projector layers of the SSL frameworks of the teacher and student encoders, respectively. s_θ^{enc} and s_ϵ^{enc} are the semantic grouping layers of the SSL frameworks of the teacher and student encoders, respectively. j^{enc} is the encoder predictor slot. g_θ and g_ϵ represent teacher and student decoders, respectively. p_θ^{dec} and p_ϵ^{dec} are the projector layers of the SSL frameworks of the teacher and student decoders, respectively. s_θ^{dec} and s_ϵ^{dec} are the semantic grouping layers of the SSL frameworks of the teacher and student decoders, respectively. j^{dec} is the decoder predictor slot.

Table 1. Performance comparison with state-of-the-art models pre-trained on COCO. We only transferred the encoder for downstream tasks. We averaged fine-tuning results over three runs. †: Collected from PixCon paper. ‡: Full re-implementation. We picked the best performing DeCon-ML-FPN ($\alpha = 0$, $dropout = 0.5$) and DeCon-SL-FCN ($\alpha = 0.25$) adaptation of SlotCon. As we are adapting SlotCon, we are in the same type of SlotCon framework (region level).

Method	Type	Object Detection VOC			Object Detection COCO			Instance Seg. COCO			Semantic Seg. VOC City	
		AP	AP50	AP75	AP	AP50	AP75	AP	AP50	AP75	mIoU	mIoU
Random init.†	-	32.8	59.0	31.6	32.8	50.9	35.3	29.9	47.9	32.0	39.5	65.3
MoCo-v2‡	Image	54.7	81.0	60.6	38.5	58.1	42.1	34.8	55.3	37.3	69.2	73.8
BYOL†		55.7	81.8	61.6	39.5	59.4	43.3	35.6	56.6	38.2	70.2	75.3
MoCo-v2+‡		54.6	81.4	60.5	39.8	59.7	43.6	35.9	57.0	38.5	71.1	75.6
ORL†	Region	55.8	82.1	62.3	40.2	60.0	44.3	36.4	57.4	38.8	70.7	75.4
PixPro†		-	-	-	40.5	60.5	44.0	36.6	57.8	39.0	72.0	75.2
DetCon†		-	-	-	39.8	59.5	43.5	35.9	56.4	38.7	70.2	76.1
UniVIP†		56.5	82.3	62.6	40.8	-	-	36.8	-	-	-	-
Odin†		56.9	82.4	63.3	40.4	60.4	44.6	36.6	57.5	39.3	70.8	75.7
DenseSiam†		55.5	81.1	61.5	-	-	-	-	-	-	-	-
Slotcon‡		55.16	81.76	61.23	40.81	60.95	44.37	36.80	57.98	39.54	71.50	75.95
DenseCL (65536 queue)†	Pixel	56.7	81.7	63.0	39.6	59.3	43.3	35.7	56.5	38.4	71.6	75.8
PixCon-SR†		57.55	82.83	64.04	40.81	60.97	44.80	36.84	57.93	39.62	72.95	76.62
DeCon-ML-SlotCon-FPN [ours]	Region	55.70	81.91	62.07	41.18	61.38	44.91	37.12	58.35	39.94	72.92	76.45
DeCon-SL-SlotCon-FCN [ours]		-	-	-	-	-	-	-	-	-	73.01	76.21

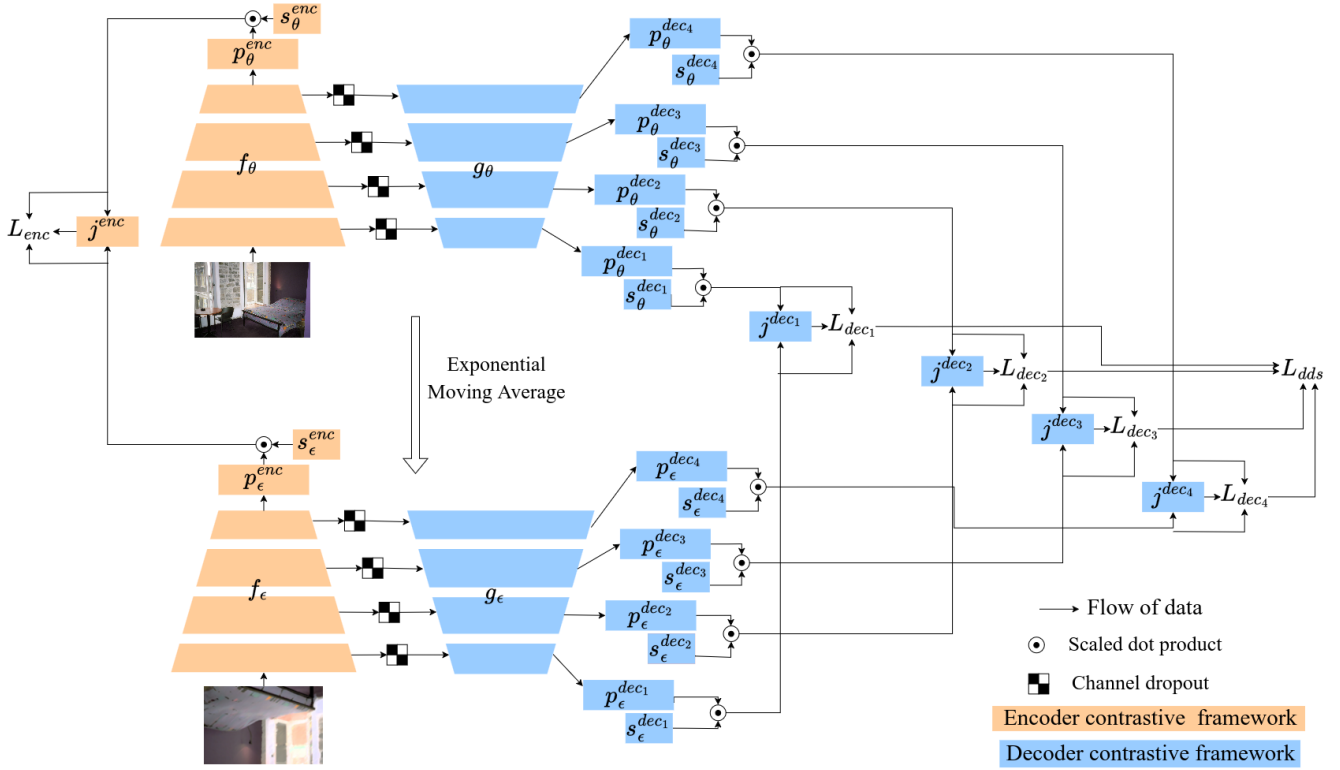


Figure 2. This schema illustrates the DeCon-ML adaptation of SlotCon framework with an FPN decoder. It also depicts the proposed decoder deep supervision and channel dropout. f_θ and f_ϵ represent teacher and student encoders, respectively. p_θ^{enc} and p_ϵ^{enc} are the projector layers of the SSL frameworks of the teacher and student encoders, respectively. s_θ^{enc} and s_ϵ^{enc} are the semantic grouping layers of the SSL frameworks of the teacher and student encoders, respectively. j^{enc} is the encoder predictor slot. g_θ and g_ϵ represent teacher and student decoders, respectively. $p_\theta^{dec_i}$ and $p_\epsilon^{dec_i}$ are the projector layers of the SSL frameworks of the teacher and student decoders, respectively. $s_\theta^{dec_i}$ and $s_\epsilon^{dec_i}$ are the semantic grouping layers of the SSL frameworks of the teacher and student decoders, respectively. j^{dec} is the decoder predictor slot.

Table 2. **Decoder specific hyperparameter tuning.** We experiment on the number of prototypes to be used for the decoder pre-training in DeCon-SL adaptation. α is fixed to 0.5 and the number of prototypes used to compute the encoder loss is fixed to 256. We report the fine-tuning mIoU as an average over three runs.

Dataset	SSL	Loss		Transfer		Number of Dec. Prototypes					
		L_{enc}	L_{dec}	enc	dec	0	64	128	256	384	512
VOC	SlotCon	✓	✗	✓	✗	71.50	-	-	-	-	-
	DeCon-CL	✓	✓	✓	✓	-	72.10	71.95	72.42	72.43	72.32
City	SlotCon	✓	✗	✓	✗	75.95	-	-	-	-	-
	DeCon-CL	✓	✓	✓	✓	-	75.67	75.79	75.67	75.87	75.97

Table 3. **Pre-training parameters count, GPU setup, and time required per epoch.** We study various pre-training setups on the COCO dataset using the SlotCon framework. Module sizes are given in millions of parameters.

Pre-training	Enc. size	Dec. size	Enc. Aux. Layers Size	Dec. Aux. Layers Size	Full Archi. Size	GPU setup	Time per epoch (s)
SlotCon	23.51 x 2	0	71.51	0	118.52	A100 80GB	255
DeCon-SL-FCN	23.51 x 2	5.31 x 2	71.51	56.83	185.97	A100 80GB	300
DeCon-SL-FPN	23.51 x 2	1.58 x 2	71.51	56.83	178.5	8 * H100 80GB	120
DeCon-ML-FPN	23.51 x 2	3.35 x 2	71.51	227.31	352.53	8 * H100 80GB	165